Erschienen in: Proceedings of the 28th European Photovoltaic Solar Energy Conference and Exhibition (EU PVSEC 2013) ; Paris, France ; conference 30 September - 04 October 2013. - München : WIP, 2013. - S. 1148-1151. - ISBN 3-936338-33-7
https://dx.doi.org/10.4229/28thEUPVSEC2013-2BV.1.36

HIGHLY EFFICIENT MULTI-BUSBAR SOLAR CELLS WITH AG NANO-PARTICLE FRONT SIDE METALLIZATION

Stefan Braun[1], Robin Nissler[2], Dirk Habermann[2], Giso Hahn[1]
[1]University of Konstanz, Department of Physics, 78457 Konstanz, Germany
[2]Gebr. Schmid GmbH&Co, Robert-Bosch-Str. 32-34, 72250 Freudenstadt, Germany

ABSTRACT: The main target for a commercially successful solar cell production is to decrease the cost/Watt-peak ratio. In the last years new techniques like fine line screen printing or plating of the front electrode entered the market. These new techniques enable a reduction of Ag or Ag containing paste of the front grid or even a substitution of this metal. Cu is a suited candidate because of its high conductivity and low price. But one should always keep in mind its high diffusivity and the associated risk of shunting the space charge region of the semiconductor device.
In this work an advanced cell design with 15 round wires instead of the widely used 3-busbars and an Ag plated front metal grid is presented, leading to efficiencies of up to 19.6% for large area p-type Cz silicon solar cells with full Al BSF. This advanced cell design combines high efficiencies and low Ag consumption not only on cell, but also on module level. In addition, the Ag rear side pads which are essential for cell interconnection should be replaced by direct Sn deposition on the screen printed Al rear side. Hereby the amount of Ag needed for the solar cell metallization could be further reduced.
Keywords: multi-busbar. Ag plating, metallization, cost reduction

1 INTRODUCTION

The need for highly efficient solar cells at low cost level led to several new metallization approaches of the front grid in the last years [1-5]. These new attempts result in narrow finger width and therefore higher currents of the solar cells. At the same time the amount of metal needed for the front side metallization is reduced. In general two different approaches can be observed.

The first one is to improve the existing technology for front side metallization. These attempts lead to fine line, dual screen printing, double screen sprinting or stencil Ag printing. Over the years a reduction in busbar width was also possible because of alignment improvements and optimized soldering parameters.

The second approach are seed and plate techniques where shallow seed layers are deposited on the front surface, co-fired to form a contact to the emitter structure, and successively strengthened via plating. Light induced Ag plating is commonly used for this technique but a Ni/Cu/Sn deposition is also possible. Cu provides a sufficient conductivity just like Ag and is much cheaper, but it also is highly diffusive [6] and one has to protect the semiconductor device with an additional metal layer. Usually electro- or electroless plated Ni layers are used as diffusion barriers. For increased adhesion abilities Ni layers are often soldered to form a nickel silicide. Theses silicides also offer very low contact resistivity. To prevent the oxidation of the plated Cu, in addition the layer has to capped with Sn. This makes Ni/Cu/Sn plating an extensive process.

A third approach which should be briefly mentioned here, are so called direct plating techniques. Here the SiN_x:H layer is opened via etching or laser ablation and metal is plated into the openings [7].

The new approach discussed in this paper is to optimize the front grid design not only by means of metal consumption, but also the efficiency gain is taken into account. Therefore, an Ag containing nano-particle ink is deposited via inkjet printing on the SiN_x:H layer of the front side. After a co-firing step the narrow seed layer is strengthened via light induced Ag plating. The amount of Ag needed for a sufficient lateral conductivity of the metal layer depends on the number of busbars of the cell structure. Increasing the amount of busbars reduces the amount of Ag needed for the finger metallization in general, because the finger length is reduced. Unfortunately, busbars and fingers are plated at the same time because since structures are located on the surface of the solar cell. By decoupling the busbars from the front side grid it is possible to separately plate the finger structure. The busbars are exchanged by Sn coated copper wires which provide excellent conductivity. In the same time the shaded area is reduced because of the round shape of the wires, especially under module conditions after encapsulation [8].

In addition the module performance can be increased using a multi-busbar cell design because the total series resistance of the interconnected structure is reduced [3].

2 SOLAR CELL PROCESSING SEQUENCE

For the experiment 6 inch alkaline textured B-doped silicon Cz material with a base resistivity of 2 Ωcm is used. The wafers are cleaned in diluted HCl and obtained a diluted HF dip before emitter diffusion in a $POCl_3$ furnace. The sheet resistance is 55 Ω/sq. To form a selective emitter structure all cells are masked by inkjet printing and the remaining emitter is etched back to 110 Ω/sq. [9]. A SiN_x:H layer is deposited and the wafer rear side obtain a full screen printed Al layer. The wafers are divided into three groups. Group 1 is the dual Ag screen printed group, group 2 and 3 wafers are Ag plated.

For the experiment an advanced multi-busbar cell design is chosen. The fingers of the multi-busbar solar cells are not continuous, they deliberately obtain finger interruptions to decrease the shaded area and surplus save Ag. In addition the number of pads is reduced which also decreases the shaded area and Ag consumption.

In Fig 1a) the unit cell of the front grid is visible. In blue the selective emitter structure is indicated. Marked in black is the finger structure which has to be printed first. It forms the contact to the emitter structure. In Fig 1b) the second printing step is presented. Marked in brown a second Ag paste was used which interconnects the finger structure with the pad, but does not form a contact to the emitter structure. In this way the contact area to the emitter is reduced which should lead to higher open circuit voltages.

Konstanzer Online-Publikations-System (KOPS)
URL: http://nbn-resolving.de/urn:nbn:de:bsz:352-252592

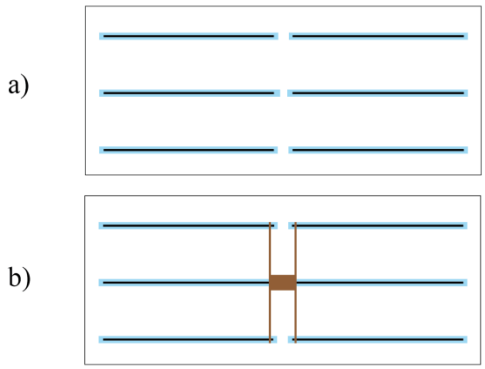

Figure 1: Unit cell of the printed front grid; a) in blue the selective emitter structure is visible, dashed fingers are marked in black; b) the second printing step interconnects the finger structure

For the second group the same pattern was chosen, but the front side metallization changed. Using an inkjet printer it was possible to deposit a narrow Ag nano-particle seed layer which was co-fired and strengthened afterwards via light induced Ag plating LIP.

The third group is the 3-busbar reference group which is also plated. To have a competitive 3-busbar design the busbar width is reduced to 1.2 mm.

All solar cells are co-fired in a belt furnace. Group 2 and 3 cells are light induced plated (LIP) with Ag. For a better understanding all groups with their key properties are displayed in Table I.

Table I: Key properties of all groups

	Group 1	Group 2	Group 3
Design	Multi-busbar	Multi-busbar	3-busbars
Front side metallization	Dual screen printing	Ag inkjet seedlayer	Ag inkjet seedlayer
		Ag LIP baselayer	Ag LIP baselayer

Finally the IV characteristic of all solar cells was determined with a Halm flasher which fully contacted the rear side of the cells.

3 RESULTS

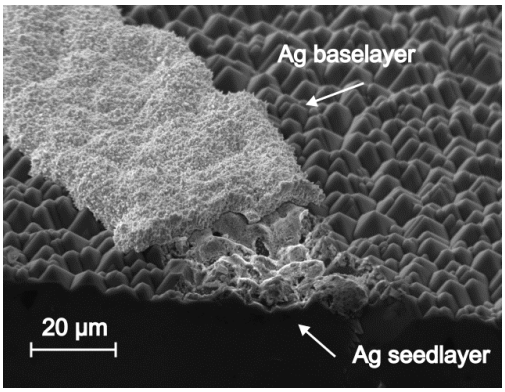

Figure 2: SEM image of an inkjet printed Ag nano-particle seedlayer on a textured surface strengthened via Ag light induced plating

Scanning electron microscope (SEM) investigations of the Ag seed- and baselayer are presented in Fig. 2. A narrow seedlayer of approx. 25-35 µm width and an Ag baselayer of approx. 30-40 µm width guarantee sufficient line conductivity for a multi-busbar solar cell design with 15 wires.

The total amount of paste, ink and metal for the front side metallization is presented in Table II.

Table II: Total amount of metal consumption for front side metallization

	Group 1	Group 2	Group 3
Screen printing	30-33 mg finger paste		
	30-32 mm pad paste		
Seedlayer		8-9 mg	11-12 mg
Baselayer		20-25 mg	85-90 mg
Total	**60-65 mg**	**28-34 mg**	**96-102 mg**

Comparing group 1 (screen printed multi-busbar cells) with the plated multi-busbar solar cells a difference in Ag mass of about 30 mg can be detected. For the dual screen printed solar cells the amount of Ag printed is still twice as high as for group 2 cells. About 30-33 mg is needed for the fingers and 30-32 mg is used for the pad structure with the interconnection fingers. This is firstly related to the fact that the width of the screen printed fingers was in the range of 50 µm, but secondly caused by the corrugated shape of a screen printed finger and the mesh used for the printing process. A further reduction of metal paste would not lead to lower efficiencies, but is currently limited by the available printing technology.

For the reference group a combined amount of about 100 mg Ag was used, which is nearly twice as much as for the screen printed multi-busbar solar cells of group 1 and three times more as for the plated multi-busbar cells. To reach a sufficiently low series resistance the 25 mm distant fingers of the 3-busbar solar cells need much more Ag, whereas the finger length of the multi-busbar solar cells was only 4.2-6 mm. For such a small finger length only 20-25 mg of Ag is needed to reach sufficient conductivity.

The results of the IV measurement are summarized in the following Figures 3-6. For current calibration of the multi-busbar solar cells a sister cell of a multi-busbar cell calibrated at ISE Callab was used for reference. Group 1 cells are marked in blue, group 2 in black and group 3 in red.

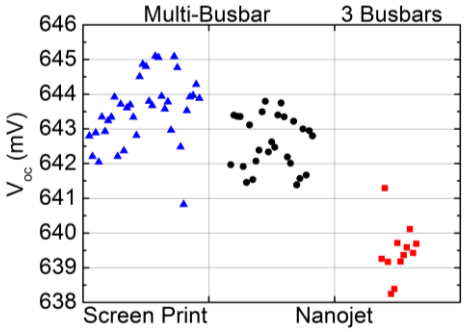

Figure 3: Open circuit voltages of the 3 groups. Advantage in voltage for group 1 can be seen because of dual printing.

One can see clearly that the highest voltages are reached in group 1 with a maximum of 645 mV. This can be related to the fact that the area of the selective emitter is reduced, because the region where the pad paste is printed is not highly doped and could be etched back which results in less recombination. For group 2 and 3 in the pad / busbar region the highly doped emitter was needed to avoid shunting.

The current densities in Fig. 4 reveal the beneficial effects of a plated front side. With a plated multi-busbar grid current densities of up to 38.3 mA/cm² could be reached. The screen printed multi-busbar solar cells show lower current densities because of increased shading related to wider fingers as mentioned above. The reference group can compete with the screen printed group because of the narrow busbars and the plated front grid.

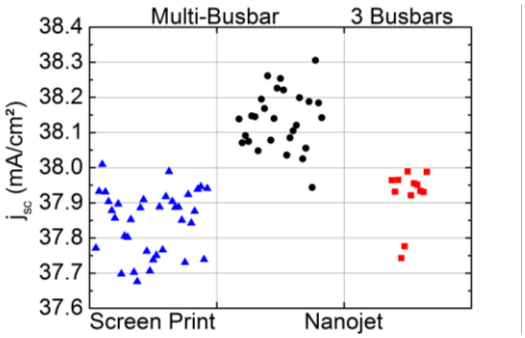

Figure 4: Current densities of the 3 groups. The plated multi-busbar solar cells obtain the highest currents.

The fill factors of all three groups are in a high range, but it is mentioned here that the alignment of these structures can be challenging. The wide spread of over $1\%_{abs}$ gives a hint that for some cells a partial misalignment could have led to reduced fill factors. The presence of high fill factors also demonstrates that the amount of plated Ag was sufficient.

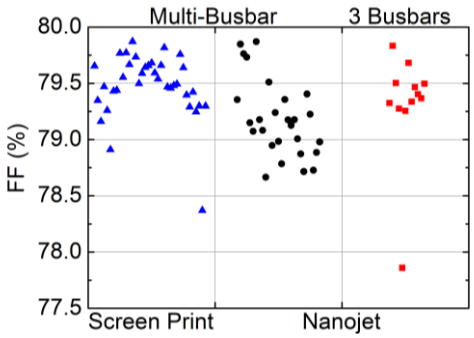

Figure 5: Fill factors results of the 3 groups. High values but a relatively wide spread for all groups.

Finally, the efficiencies are presented in Fig 6. All three groups show high efficiencies. The highest efficiency of group 1 is 19.5%, for group 2 it is even slightly higher with 19.6%, and the best cell of group 3 reaches 19.4%.

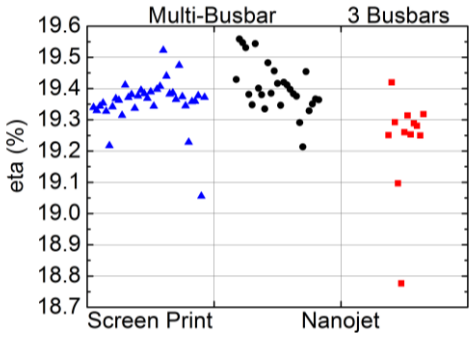

Figure 6: Solar cell efficiencies of the three groups. Highest efficiencies reached with plated front grid and multi-busbar front electrode (see Table II).

All three groups show efficiencies in the same range, but note that the amount of Ag needed for the front side metallization varies strongly.

4 CONCLUSION

The optimized multi-busbar solar cell design with one pad for three fingers and interruptions in the finger grid demonstrates its advantages compared to the 3-busbar solar cell design. The efficiencies are slightly higher, but the main advantage is the Ag reduction that was reached by using a seed and plate approach. A significant Ag reduction can be achieved with about 40 mg for a dual screen printed multi-busbar solar cell and even 70 mg for the plated multi-busbar solar cells compared to the 3-busbar reference cells leading to significant cost reduction. High fill factors indicate that the amount of Ag plated was sufficient. Efficiencies of 19.4% could be reached with a 3-busbar selective emitter solar cell design. The highest efficiency for a multi-busbar solar cell was 19.6%.

5 OUTLOOK

An optimized alignment and a narrower distribution in fill factor should lead to more homogeneous results. In a next step the new cell design could prove the even higher performance on module level compared to a 3-busbar cell design as was reported earlier [9]. For the interconnection on the rear side, an approach without Ag pads [10] can lead to promising results on module level without changing the cell design. The next generation of inkjet printheads will provide even finer lines and can easily be integrated in a running inkjet system.

A next generation of cell design optimization could investigate the use of Ni instead of Ag, because high finger conductivities are not necessary for the multi-busbar cell design. Also dielectric layers could be easily integrated in such a solar cell concept.

5 AKNOWLEDGEMENTS

The authors would like to thank L. Mahlstaedt and A. Dastgheib-Shirazi and the engineering team of the company Schmid for the support as well as the company Gebr. Schmid GmbH for the funding of this project.

6 REFERENCES

[1] D. Kray, N. Bay, G. Cimiotti, N. Fritz, M. Glatthaar, S. Kleinschmidt, A. Lösel, O. Lühn, J. Schramm-Moura, A. Rodofili, A. Träger, H. Kühnlein, H. Nussbaumer, Proc. 26th EUPVSEC, Hamburg, pp. 1199-1202, 2012.

[2] A. Schneider, L. Rubin, G. Rubin, Proc. 4th WC PEC, Waikoloa, pp. 1095-1098, 2006.

[3] S. Braun, G. Micard, G. Hahn, Energy Procedia 27 (2012) 227.

[4] A. Mette, New concepts for front side metallization of industrial silicon solar cells, Dissertation University of Freiburg, 2007.

[5] M. Hörteis, J. Bartsch, S. Binder, A. Filipovic, J Merkel, V. Radtke, S.W. Glunz, " Progress in Photovoltaics: Research and Applications 18 (2010) 240.

[6] A. Fick, Annalen der Physik 170(1) (1855) 59.

[7] L Tous, J-F. Lerat, T. Emeraud, R. Negru, K. Huet, A. Uruena, M. Aleman, J. Meersschaut, H. Bender, R. Russell, J. John, J. Poortmans, R. Mertens, Progress in Photovoltaics: Research and Applications 21 (2012) 267.

[8] A.W. Blakers, Journal of Applied Physics 71(10) (1992) 5237.

[9] H. Haverkamp, A. Dastgheib-Shirazi, B. Raabe, F. Book, G. Hahn, Proc. 33rd IEEE PVSC, San Diego, pp. 430-433, 2008.

[10]S. Braun, G. Hahn, R. Nissler, C. Pönisch, D. Habermann, Energy Procedia 38 (2013) 334.

[11] H. v. Campe, S. Huber, S. Meyer, S. Reif, J. Vietor, Proc. 27th EUPVSEC, Frankfurt, pp. 1150-1153, 2012.